Chinese Journal of Natural Medicines

Honokiol attenuates diabetes by enriching *Akkermansia muciniphila* andregulating tryptophan metabolism in mice

Yang Lin, Zhengmeng Jiang, Zhilu Yu, Tianqing Huang, Wanyu Gui, Ziyuan Wang, Fei Li, Pingting Xiao, Changyin Li, Ehu Liu

Citation: Yang Lin, Zhengmeng Jiang, Zhilu Yu, Tianqing Huang, Wanyu Gui, Ziyuan Wang, Fei Li, Pingting Xiao, Changyin Li, Ehu Liu, Honokiol attenuates diabetes by enriching *Akkermansia muciniphila* andregulating tryptophan metabolism in mice, Chinese Journal of Natural Medicines, 2026, 24(1), 59−72. doi: 10.1016/S1875−5364(26)61077−1.

View online: https://doi.org/10.1016/S1875−5364(26)61077−1

Chinese Journal of Natural Medicines 24 (2026) 59-72

Contents lists available at ScienceDirect

Chinese Journal of Natural Medicines

journal homepage: www.cjnmcpu.com/

Original article

Honokiol attenuates diabetes by enriching *Akkermansia muciniphila* andregulating tryptophan metabolism in mice

Yang Lin[a,Δ], Zhengmeng Jiang[b,Δ], Zhilu Yu[a,Δ], Tianqing Huang[a], Wanyu Gui[c], Ziyuan Wang[d], Fei Li[a,*], Pingting Xiao[a,*], Changyin Li[c,*], Ehu Liu[a, b,*]

[a] *State Key Laboratory of Natural Medicines, China Pharmaceutical University, Nanjing 211198, China*
[b] *School of Pharmacy, Nanjing University of Chinese Medicine, Nanjing 210023, China*
[c] *Department of Clinical Pharmacology, Jiangsu Province Hospital of Chinese Medicine, Affiliated Hospital of Nanjing University of Chinese Medicine, Nanjing 210029, China*
[d] *Center for Analysis and Testing, Public Experimental Platform, China Pharmaceutical University, Nanjing 211198, China*

ARTICLE INFO

Article history:
Received 28 January 2025
Revised 4 April 2025
Accepted 9 June 2025
Available online 20 January 2026

Keywords:
Honokiol
Diabetes mellitus
Akkermansia muciniphila
Tryptamine
Aryl hydrocarbon receptor

ABSTRACT

Diabetes mellitus (DM) is a chronic disease influenced by gut microbiome disturbances. Honokiol (HON), a low oral bioavailability compound from *Magnolia officinalis* bark, has demonstrated potential as a treatment for DM. This research investigates the effects of HON on gut microbiota and host metabolism to elucidate its mechanism of action in DM. After 8 weeks of intervention through fecal microbiota transplantation (FMT) or antibiotic treatment, HON improved glucose tolerance and lipid metabolism in a gut microbiota-dependent manner. Specifically, HON administration significantly increased *Akkermansia muciniphila* (AKK) abundance and modulated tryptophan (TRP) metabolism, as evidenced by 16S ribosomal ribonucleic acid (rRNA) gene sequencing and untargeted/targeted metabolomics analysis. Notably, research revealed that AKK metabolized TRP into tryptamine (TA) and other metabolites *in vitro*. Both AKK and TA activated the aryl hydrocarbon receptor (AHR) pathway, increasing circulating glucagon-like peptide-1 (GLP-1) levels and ameliorating diabetes-related symptoms in DM mice. These findings indicate that HON's hypoglycemic effect primarily stems from AHR-GLP-1 pathway activation through targeted modulation of AKK and microbial TRP metabolite TA, potentially enhancing HON's clinical applications.

1. Introduction

Diabetes mellitus (DM) represents a significant global public health challenge due to its increasing prevalence and complex pathogenesis [1, 2]. Unmanaged DM significantly impacts human health and quality of life by increasing the risk of renal, cardiovascular, and liver diseases [3]. Contemporary pharmaceutical treatments for DM, including metformin, liraglutide, and sulfonylurea, may produce adverse effects such as gastrointestinal complications and weight loss [4]. Therefore, developing more effective anti-DM medications from medicinal plants with reduced side effects remains a priority.

Recent studies have identified alterations in gut microbiota composition in both DM patients and animal models [5, 6]. The gut microbiota plays a crucial role in diabetes development and progression [7]. Disruptions in intestinal microbiota can trigger bacterial endotoxin lipopolysaccharide (LPS) leakage, leading to mucosal barrier dysfunction and subsequent glucose metabolism disturbances [1]. Fecal microbiota transplantation (FMT) studies have demonstrated that microbiota from healthy donors improves glucose tolerance in diabetic mice [8-10]. *Akkermansia muciniphila* (AKK), a mucin-degrading bacterium maintaining glucose homeostasis, shows increased presence in diabetic individuals receiving dietary fiber or metformin [11, 12]. These findings emphasize intestinal microbiota as a promising therapeutic target for DM.

Metabolomics serves as a critical method for identifying endogenous differential metabolites, offering insights into disease mechanisms [13]. The gut microbiota processes dietary components and breaks down host-derived substances to generate various metabolites, which function as essential mediators in gut microbiota-host interactions [14]. The integration of metabolomics and microbiology techniques facilitates understanding of how drugs improve diabetes through the gut-metabolites-brain axis [15] or the gut-metabolites-liver axis [16].

Magnolia extracts serve as nutritional supplements in the United States, recognized for their cardiovascular protective, anti-obesity, anti-inflammatory, and anti-tumor properties [17-19]. The extract from *Magnolia officinalis* bark has been utilized in traditional Chinese medicine as Houpo for treating gastrointestinal disorders for millennia [20]. Honokiol (HON), the primary bioactive compound and quality control component of Houpo, demonstrates the capacity to reduce blood glucose, protect pancreatic β cells, and improve insulin resistance in high-fat diet (HFD)-streptozotocin (STZ)-induced DM mice or rats [21, 22]. Given HON's low oral bioavailability of approximately 5% [23], investigation of the

* Corresponding author.
E-mail addresses: lifei@cpu.edu.cn (F. Li); 1520210064@cpu.edu.cn (P. Xiao); fsyy00612@njucm.edu.cn (C. Li); 300641@njucm.edu.cn (E. Liu)
Δ These authors contributed equally to this work.

https://doi.org/10.1016/S1875-5364(26)61077-1

gut microbiota's role in mediating HON's effects warrants attention.

This study evaluates the hypothesis that HON ameliorates DM through modulation of gut microbiota composition and function. Initially, the investigation focused on assessing the anti-diabetic efficacy of HON using a DM mouse model induced by HFD-STZ, and examined the microbiota dependency of this effect. Subsequently, 16S ribosomal ribonucleic acid (rRNA) gene sequencing analysis, untargeted metabolomics, and targeted tryptophan (TRP) metabolic analysis were performed to elucidate alterations in both the composition and functionality of gut microbiota. The results demonstrated that HON restructures gut microbial composition, enriches the beneficial bacterium AKK, and upregulates microbial TRP metabolites, which activate the aryl hydrocarbon receptor (AHR) signaling pathway and increase glucagon-like peptide-1 (GLP-1) levels, thereby ameliorating diabetes symptoms.

2. Materials and methods

2.1. Chemicals and reagents

STZ (BS185) was obtained from Biosharp (Anhui, China). CMC-Na (C8621) was purchased from Sinopharm Chemical Reagent (Shanghai, China). HON (purity by HPLC > 98%, H111272) and corn oil (C11602) were purchased from Aladdin Scientific (Shanghai, China). Metformin hydrochloride (MET, D9351) and dimethylsulfoxide (DMSO, D8370) were purchased from Solarbio (Beijing, China). Insulin (CSP001-10) was obtained from Shanghai Zhong Qiao Xin Zhou Biotechnology (Shanghai, China). Ampicillin (A6920), neomycin (N8090), vancomycin (V8050), and metronidazole (M8060) were purchased from Solarbio (Beijing, China). 4% paraformaldehyde and Carnoy's fixative were purchased from Servicebio Technology (Wuhan, China). TRP (ZC-6369), kynurenine (KYN, ZC-46354), 5-hydroxytryptophan (5-HTP, ZT-20823), indole-3-acetic acid (IAA), indole-3-propionic acid (IPA, ZC-6030) were purchased from Shanghai ZhenZhun Biotechnology (Shanghai, China); indole-3-carboxaldehyde (I3C, Lot No. 420030-201501) was purchased from the National Institutes for Food and Drug Control (Beijing, China); tryptamine (TA, Lot. No. 21040958) was purchased from Tan-Mo Technology (Changzhou, China); TA hydrochloride (Lot No. C13070344) was purchased from Macklin (Shanghai, China). CH223191 (S80605) was purchased from Yuanye (Shanghai, China).

2.2. Animal model and treatment

All animal experiments conducted in this study were approved by the Institutional Animal Care and Use Committee of China Pharmaceutical University in Nanjing, China (No. 2019-10-007), and performed in strict accordance with their guidelines. Male C57BL/6J mice weighing between 12 and 14 g were obtained from Yangzhou University's Comparative Medicine Center. Following a one-week acclimatization period, 10 mice were randomly selected for the CHOW group and received a chow diet (total energy: 3342 kcal·kg^{-1}, Nanjing Qinglong Mountain Laboratory Animal Company), while the remaining mice received an HFD [TP23300, total energy: 5000 kcal·kg^{-1}, TROPHIC Animal Feed High-Tech. (Nantong, China)] to induce insulin resistance. After 4 weeks, STZ dissolved in 0.1 mol·L^{-1} citrate buffer (pH 4.5) was administered intraperitoneally (i.p.) (40 mg·kg^{-1}) every other day for three administrations, while mice in the CHOW group received an equivalent volume of citrate buffer. Fasting blood glucose (FBG) measurements were conducted at 5 and 7 d after the final injection, and mice with FBG exceeding 11.1 mmol·L^{-1} were classified as DM mice [24].

2.3. Evaluation of the anti-diabetic effect of HON in DM mice

To assess the anti-diabetic effect of HON, 50 DM mice were randomly divided into five groups and received HFD diets along with intragastric administration (i.g.) of 0.5% CMC-Na (Model groups, DM), 50 mg·kg^{-1} of HON (HON-L), 100 mg·kg^{-1} of HON (HON-M), 200 mg·kg^{-1} of HON (HON-H), and 200 mg·kg^{-1} of MET for 8 weeks, while 10 CON group mice received chow diets and an equivalent volume of 0.5% CMC-Na solution.

2.4. Oral glucose tolerance test (OGTT) and insulin tolerance test (ITT)

During the final week, mice received a glucose solution (2 g·kg^{-1}) orally after overnight fasting in the OGTT experiment. For the ITT experiment, mice underwent 6 h fasting before receiving 0.75 IU·kg^{-1} insulin (i.p.). Blood samples from the tail vein were used to measure glucose levels at 0, 30, 60, 90, and 120 min following glucose or insulin administration. The OGTT and ITT data were quantified using the area under the curve (AUC) formula.

2.5. Serum biochemical measurements

Commercial kits from Nanjing Jiancheng Bioengineering Institute were used to measure serum total cholesterol (TC), serum total triglyceride (TG), serum high-density lipoprotein cholesterol (HDL-C), and serum low-density lipoprotein cholesterol (LDL-C). Fast serum insulin and LPS were measured using commercially available enzyme-linked immunosorbent assay (ELISA) kits (Mlbio, Shanghai, China) according to manufacturer guidelines. Homeostasis model assessment values for insulin resistance (HOMA-IR) = (FBG × fasting insulin)/22.5 [25].

2.6. Histopathological analysis

Pancreatic, epididymal adipose, and hepatic tissues were fixed in 4% paraformaldehyde, while colon tissue was fixed in Carnoy's fluid. Hematoxylin and eosin (H&E) staining, alcian blue staining, or immunohistochemistry for various tissues were performed by Servicebio Technology (Wuhan, China). Section evaluation was performed using a scanner (NanoZoomer 2.0 RS, Hamamatsu, Japan). Adipose tissue images were analyzed according to previously described methods [26].

2.7. Gene expression

Colon total RNA extraction and complementary deoxyribonucleic acid (cDNA) synthesis were performed using TRIzol reagent and cDNA reverse transcription kit (Vazyme, Nanjing, China), respectively. Quantitative real-time polymerase chain reaction (qPCR) was performed using the Roche LightCycler 96 System and SYBR Green (Vazyme). Samples were analyzed in duplicate using 96-well reaction plates (Roche). The relative messenger ribonucleic acid (mRNA) expressions of target genes were calculated using the $2^{-\Delta\Delta CT}$ method and normalized to housekeeping genes *Gapdh* or *Rpl19*. Primer sequences are shown in Table S1.

2.8. FMT and antibiotic treatment

FMT was conducted over the 8-week intervention period following established protocols [27]. Prior to FMT, recipient mice's endogenous microbiota was eliminated using an antibiotic cocktail (ABS) containing ampicillin (1 g·L^{-1}), neomycin (0.5 g·L^{-1}), vancomycin (0.5 g·L^{-1}), and metronidazole (1 g·L^{-1}), administered daily by oral gavage for three consecutive days. Daily fecal samples from donors in different groups (DM, HON) were collected

throughout the 8 weeks. Fresh feces were suspended in sterile phosphate-buffered saline (PBS) at 100 mg·mL^{-1}. The mixture was centrifuged at 2000 r·min^{-1} for 5 min to obtain the supernatant for transplantation, prepared within 10 min of gavage. For *in vivo* antibiotic treatment, HFD-STZ-induced mice received ABS in drinking water for 8 weeks.

2.9. Gut microbiota analysis

Gut microbiota analysis was performed by Majorbio (Shanghai, China) using high-throughput 16S rRNA gene sequencing. Raw sequence data analysis followed the method described by Jiang et al. [27]. The operational taxonomic units (OTUs) table and Shannon index were generated using QIIME to measure α-diversity. Principal coordinate analysis (PCoA) was employed to assess microbial community clustering (β-diversity). Linear discriminant analysis (LDA) effect size (LEfSe) analysis identified differentiating taxa of biological relevance between groups. Redundancy analysis (RDA) evaluated correlations between DM symptoms and bacterial genera.

2.10. Fecal DNA extraction and relative quantification

Fecal DNA extraction followed previously described methods [28]. Specific primers were used for qPCR analysis to quantify AKK in fecal samples (Table S1). Sample cycle threshold values were compared against a standard curve (Table S2), generated in duplicate using diluted genomic DNA from AKK. Results are expressed as (Log_{10} DNA copies)/g feces.

2.11. Evaluation of the anti-diabetic effect of AKK in DM mice

The cultures were centrifuged at 2000 r·min^{-1} for 5 min prior to bacterial administration. The sediment was resuspended with PBS and administered to the AKK group of mice *via* oral gavage at a concentration of 1 × 10^8 colony-forming units (CFUs) of bacteria. CON or DM mice received an equivalent volume of PBS.

2.12. The effect of HON and TRP on AKK in vitro

Fecal samples from CON mice were prepared in a 10% PBS suspension to examine changes in AKK abundance within fecal microbiota. HON was introduced at final concentrations of 5, 10, and 20 μmol·L^{-1}. The final concentrations of TRP were 0.2, 0.4, and 0.8 g·L^{-1}, respectively. Cultures were maintained for 36 h using Shanghai Yuejin Company's anaerobic incubation apparatus. Following cultivation, bacteria were isolated by centrifugation at 12 000 r·min^{-1} for 20 min. The direct effects of HON or TRP on AKK proliferation were evaluated using qPCR. AKK (BNCC 341917) was cultured anaerobically in BHI broth (Oxoid, Basingstoke, UK) supplemented with 0.05% porcine mucin and 0.1% cysteine to examine direct effects. AKK quantification followed established protocols [29]. HON (5, 10, and 20 μmol·L^{-1}) or TRP (0.2, 0.4, and 0.8 g·L^{-1}) were added to the culture medium at varying concentrations. After appropriate incubation periods, bacterial growth was assessed by measuring optical density at 600 nm (OD_{600}). All experiments were performed in triplicate.

2.13. Metabolomics profiling analysis

Serum analysis using ultrahigh-performance liquid chromatography quadrupole time-of-flight mass spectrometry (UPLC-QTOF/MS) followed protocols described in HILIC Metabolomics Profiling [30]. Fecal preparation and analysis followed previously established methods [26]. Significant features between DM *vs* CON mice groups or DM *vs* HON groups were identified using criteria of variable importance in the projection (VIP) > 1 and $P < 0.05$. Identified differential metabolites underwent analysis using MetaboAnalyst (https://www.metaboanalyst.ca/) to identify potentially implicated KEGG pathways.

2.14. TRP metabolite target quantification

TRP metabolites were analyzed using a dynamic MRM scan mode on the LC-(AB) API 4000 MS/MS System (Table S3). Sample separation occurred at 45 °C on an Agilent Poroshell 120 SB-C_{18} column (100 mm × 3.0 mm, 2.7 μm; Agilent Technologies, CA, USA) with a flow rate of 0.4 mL·min^{-1}. The gradient-elution procedure consisted of: 0–2 min, 85% A; 2–2.1 min, 85%–62% A; 2.1–8 min, 62% A; 8–8.5 min, 62%–85% A; 8.5–13 min, 85% A. Target metabolite concentrations were quantified using calibration curves with internal standards [31,32] (Tables S4 and S5).

2.15. The effect of AKK on TRP metabolism in vitro

AKK was incubated anaerobically at 37 °C for 24 h. A 1 mL bacterial solution was collected and centrifuged at 12 000 r·min^{-1} for 10 min at 4 °C. The supernatant (100 μL) was combined with 600 μL pre-cooled methanol–acetonitrile (1∶1), followed by vortexing and centrifugation. The resulting supernatant (600 μL) underwent solvent evaporation. TRP metabolite separation and concentration analysis followed the previously described method [33].

2.16. Mouse intervention study with TA

TA (in the form of hydrochloride), an AHR agonist, was suspended in sterile PBS. The TA group received intraperitoneal administration of TA (12.5 mg·kg^{-1}) three times weekly for 8 weeks. CON and DM mice received intraperitoneal PBS injections [34].

2.17. Western blotting

Western blotting was performed according to previously described methods [35]. The primary antibodies utilized were: cytochrome P450 1A1 (CYP1A1, 1∶1000, Cat AF5312; Affinity, Changzhou, China); AHR (1∶1000, Cat A1451; Abclonal, Wuhan, China); β-actin (1∶2000, Cat AC028; Abclonal, Wuhan, China); GLP-1 (1∶1000, Cat AF0166; Affinity, Changzhou, China). HRP goat anti-rabbit IgG (H + L) (1∶2000, AS014; Abclonal, Wuhan, China) served as the secondary antibody. Band intensity on Western blotting was quantified through densitometry using Image-J software.

2.18. Mouse intervention study with AHR antagonist CH223191

The AHR antagonist CH223191 was dissolved in D9351 and DMSO and subsequently diluted in corn oil. HON group mice received oral administration of HON (200 mg·kg^{-1}·d^{-1}) for 8 weeks, while the CH223191 + HON group received additional injections of CH223191 (100 μg/mouse) three times weekly. CON mice and DM mice received intraperitoneal DMSO vehicles.

2.19. GLP-1 level quantification

Mice were fasted for 6 h, then administered sitagliptin (HY-13749, 25 mg·kg^{-1}, MCE, NJ, USA) 45 min before glucose solution (2 g·kg^{-1}). Blood samples (100 μL) were collected *via* retroorbital venipuncture 15 min after glucose gavage for serum collection. GLP-1 levels were measured using a commercial enzyme-linked immunosorbent test kit (Mlbio, Shanghai, China) [36].

For the *in vitro* study, GLP-1 secretion reduction in STC-1 cells (BNCC342403, Beijing, China) was induced by palmitic acid (PA), followed by HON or TA treatment for 24 h post-adhesion.

The medium was replaced with fresh L-Dulbecco's modified Eagle medium (DMEM, Keygen BioTECH, Nanjing, China) containing 10% FBS. After 3 h, the medium was replaced with serum-free H-DMEM (Keygen BioTECH, Nanjing, China) for 5-h incubation to stimulate hormone secretion. Supernatants underwent centrifugation at 5000 × *g* for 30 min. GLP-1 concentrations were determined using the ELISA kit (Mlbio, Shanghai, China) [37, 38].

2.20. Statistical analysis

All experimental data are expressed as mean ± standard error of the mean (SEM). Statistical analyses were performed using GraphPad Prism Version 8.0.1 (San Diego, CA, USA). Results were considered statistically significant at $P < 0.05$. For datasets containing more than two groups, one-way ANOVA followed by Dunnett's multiple comparisons test was applied.

3. Results

3.1. HON improves glucose homeostasis and lipid metabolism in DM mice

A mouse model of DM induced by HFD and STZ was utilized to investigate HON's effects on glucose homeostasis in diabetes (Figs. 1A and 1B). HFD-STZ-treated mice exhibited increased body weight, significant hyperglycemia, and elevated food and water intake (Figs. S1A–S1E), confirming successful DM model

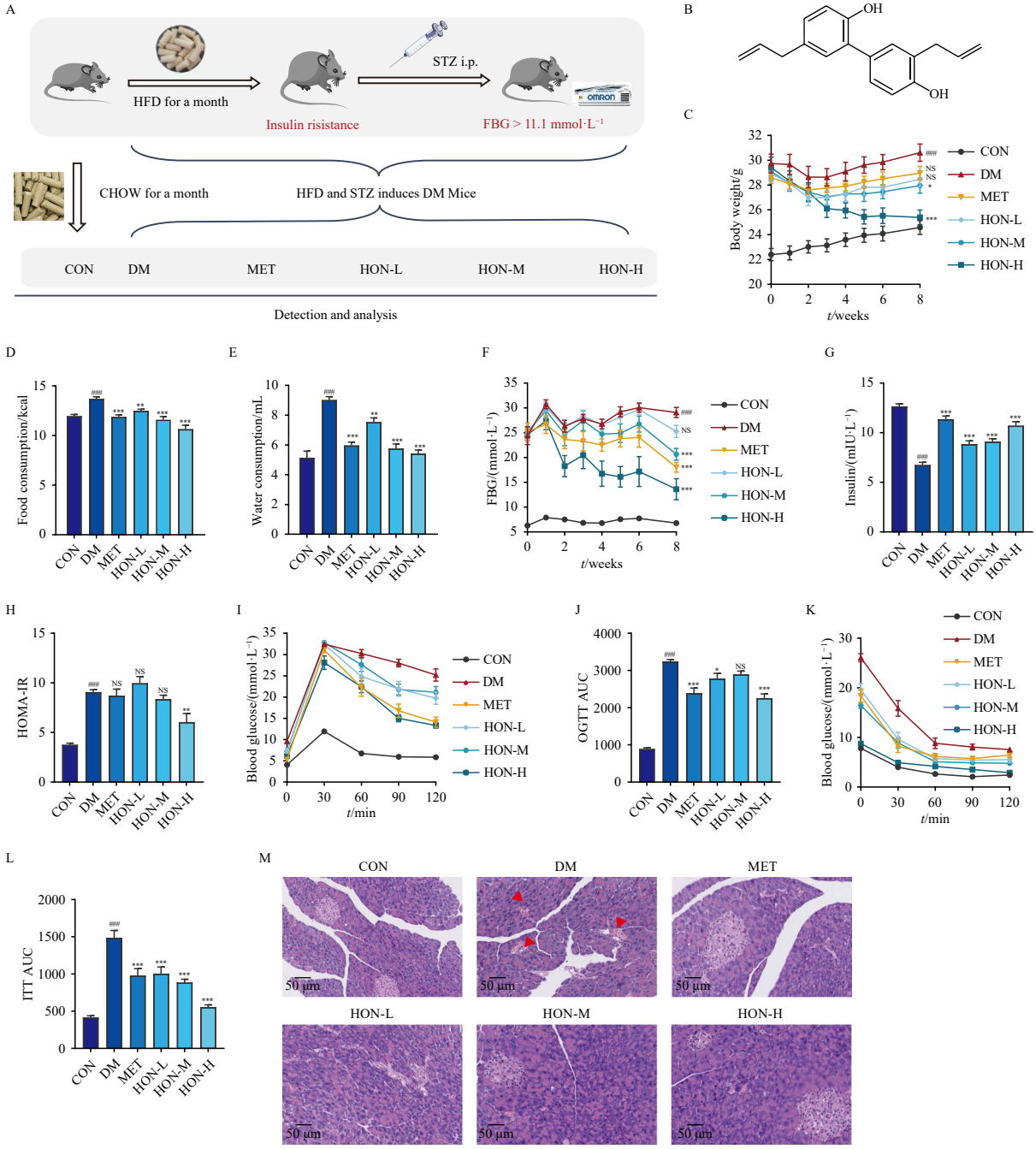

Fig. 1 HON improves glucose homeostasis in DM mice. During the 8 weeks of treatment, CON mice and DM mice were fed with a normal chow diet or HFD, respectively (n = 10). (A) Experimental protocol. (B) The chemical structure of HON. (C) Body weight curves. (D and E) Food consumption and water consumption per mouse per day. (F) FBG curves. (G) Serum insulin levels. (H) HOMA-IR levels. (I and J) Blood glucose levels in OGTT with AUC. (K and L) Blood glucose levels in ITT with AUC. (M) H&E staining of the pancreatic tissue (n = 3; scale bar, 50 μm). Data were presented as mean ± SEM. $^{\#}P < 0.05$, $^{\#\#}P < 0.01$, $^{\#\#\#}P < 0.001$ *vs* CON group; $^{*}P < 0.05$, $^{**}P < 0.01$, and $^{***}P < 0.001$ *vs* DM group; NS, no significance.

establishment. HON administration improved HFD-induced body weight gain, polyphagia, and polydipsia dose-dependently over eight weeks compared to the DM group (Figs. 1C–1E). Mice treated with HON or MET demonstrated lower fasting glucose levels and increased insulin levels compared to DM mice (Figs. 1F and 1G). The HOMA-IR index decreased following treatment with HON-H (Fig. 1H). OGTT and ITT results indicated that HON and MET reduced blood glucose levels and AUC values in diabetic mice (Figs. 1I–1L). While DM mice showed pancreatic cell reduction, atrophy, and localized necrosis in islet tissue morphology, HON therapy mitigated pancreatic damage (Fig. 1M). These findings indicate that HON treatment improves glucose tolerance, enhances insulin sensitivity, and partially restores glucose homeostasis in DM mice.

Regarding lipid metabolism, HON supplementation reduced liver index and epididymal fat index (Figs. S1F and S1G). HON and MET treatment decreased the cell size of epididymal fat tissue (Figs. S1H and S1I). The liver tissue of the DM group exhibited localized necrosis and hepatic steatosis with fat droplets, though HON partially mitigated these symptoms (Fig. S1J). Additionally, DM mice demonstrated elevated serum levels of TC, TG, LDL-C, and HDL-C compared to CON mice (Figs. S1K–S1N), while HON and MET treatment reduced the levels of TG and LDL-C in diabetic mice, indicating that HON could ameliorate the alterations in lipid metabolism in DM mice.

3.2. HON attenuates DM in a gut microbiota-dependent manner

To investigate whether the gut microbiome mediates the mechanism of HON action, microbiota from HON-treated DM mice were transferred to recipient DM mice *via* gavage daily (Fig. 2A). Following eight weeks of intragastric administration with

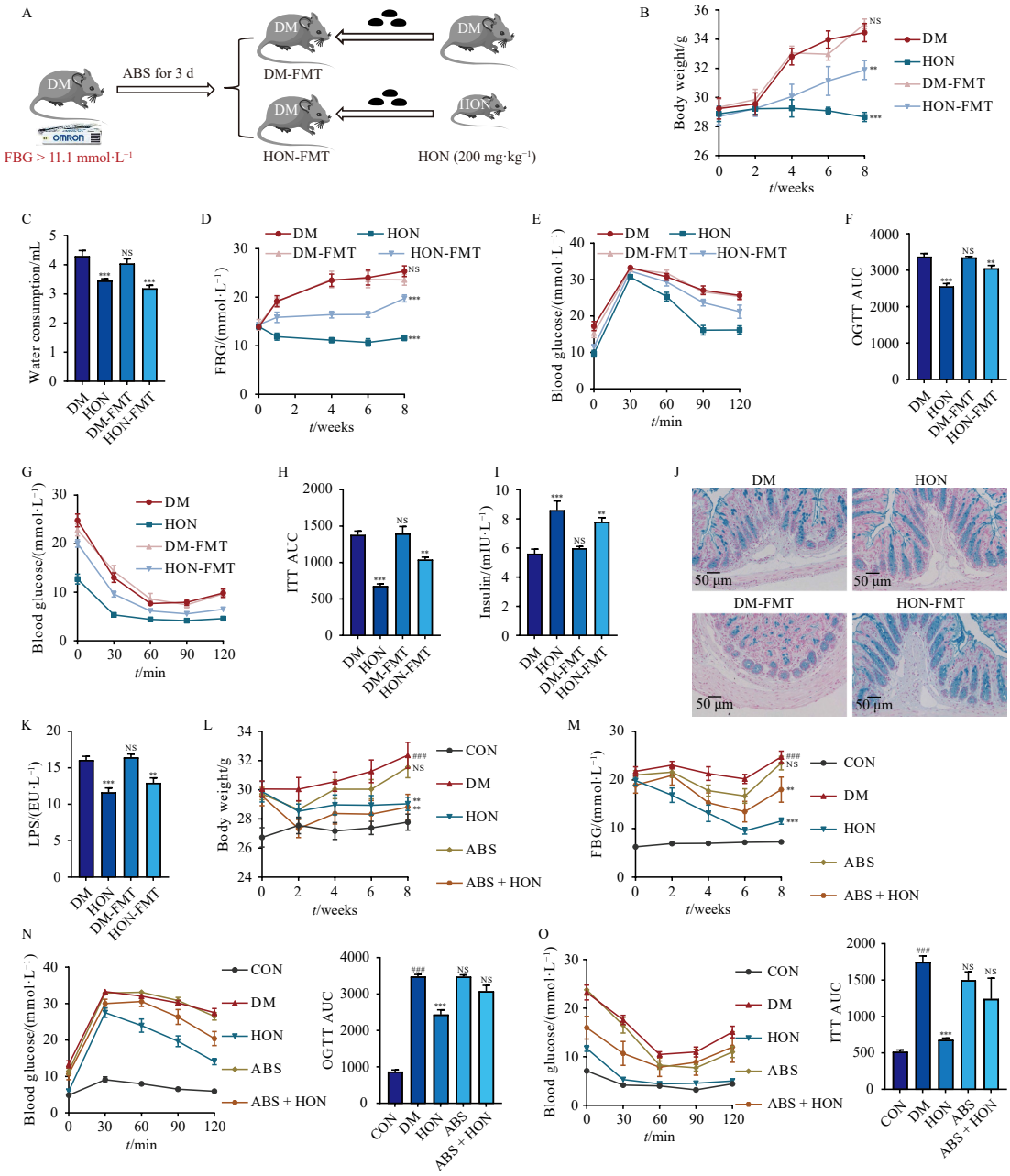

Fig. 2 The protective effects of HON on diabetes depended on fecal microbiota. During the FMT experimental period (n = 8): (A) study design of FMT; (B) body weight curve; (C) water consumption; (D) FBG curve; (E and F) blood glucose levels in OGTT with AUC; (G and H) blood glucose levels in ITT with AUC; (I) insulin levels; (J) the colon with alcian blue staining (n = 3; scale bar, 50 μm); (K) LPS levels. During the ABS experimental period (n = 8): (L and M) body weight and FBG curves; (N) blood glucose levels in OGTT with AUC; (O) blood glucose levels in ITT with AUC. Data were presented as mean ± SEM. $^{\#}P < 0.05$, $^{\#\#}P < 0.01$, $^{\#\#\#}P < 0.001$ *vs* CON group; $^{*}P < 0.05$, $^{**}P < 0.01$, and $^{***}P < 0.001$ *vs* DM group; NS, no significance.

fecal microbiota liquid, HON-FMT mice demonstrated significant reductions in body weight, water consumption, and FBG levels compared to the DM-FMT group (Figs. 2B–2D). However, FMT did not reproduce the effect on food consumption (Fig. S2A). Notably, the OGTT and ITT levels of the HON-FMT group were lower than those of the DM-FMT group, while insulin levels showed an inverse trend (Figs. 2E–2I). Furthermore, intestinal microbiota transplantation from the HON group to DM mice enhanced lipid metabolism, as evidenced by reduced liver and epididymal fat indices and decreased TG and LDL-C levels (Figs. S2B–S2E). The histomorphology of epididymal fat, liver, and pancreatic tissues in HON-FMT mice showed improvement compared to the DM-FMT group (Fig. S2F). Alcian blue staining revealed that HON treatment increased colonic epithelial mucosa thickness, and HON-FMT mice exhibited similar patterns to the HON group compared with DM-FMT mice (Fig. 2J). Additionally, HON microbiota transplantation to DM mice decreased endotoxin production (Fig. 2K). In summary, the beneficial effects of HON administration were largely transferable through gut microbiota.

To further validate that the protective effects of HON in DM mice are dependent on the gut microbiota, diabetic mice received either HON treatment alone or in combination with ABS for 8 weeks to deplete gut microbiota, followed by assessment of DM-related symptoms (Fig. S3A). As shown in Figs. 2L–2O, ABS administration significantly reduced HON's impact on body weight and blood glucose regulation. While ABS treatment demonstrated effects on food and water consumption and increased serum insulin levels, the combination of ABS + HON showed no additional benefits (Figs. S3B–S3D). The protective effects of HON on metabolic parameters and histomorphology were partially diminished in the absence of microbiota (Figs. S3E–S3I). Furthermore, ABS treatment eliminated HON's beneficial effect on the intestinal barrier (Figs. S3J–S3L). These findings suggest that HON exhibits its anti-diabetic effects through gut microbiota-dependent mechanisms.

3.3. HON reverses gut dysbiosis in DM mice

Intestinal barrier dysfunction is widely recognized as a characteristic feature of diabetes [8]. The increased mRNA expression of intestinal tight junction proteins *ZO-1*, *Occludin*, and *Claudin-1* indicated that HON enhanced gut barrier function and ameliorated colon injury (Fig. 3A). Additionally, HON supplementation decreased endotoxin LPS levels in DM mice (Fig. 3B).

High-throughput sequencing of the gut bacterial 16S rRNA gene was performed to characterize HON's effects on gut microbiota. The α-diversity values for bacterial community analysis revealed differences between HON and DM groups, demonstrated by reduced observed_OTUs and Shannon index (Figs. 3C and 3D). PCoA revealed significant intergroup differences in gut microbiota composition and abundance, with the three groups forming distinct clusters influenced by PC1 (47.3%) and PC2 (24.2%) factors (Fig. 3E). LEfSe analysis (LDA > 4) showed that the DM group was characterized by the families *Desulfovibrionaceae*, *Erysipelatoclostridiaceae*, *Erysipelotrichaceae*, and *Peptostreptococcaceae*, while the HON group exhibited predominance of *Sutterellaceae*, *Enterobacteriaceae*, and *Akkermansiaceae* families (Fig. 3F). Analysis of the top 20 genera's relative abundance revealed increased levels of *Akkermansia* at the genus level in the HON group (0.13% in CON, 3.12% in DM, and 50.26% in HON, Figs. 3G and 3H), suggesting *Akkermansia*'s potential role in HON's protective effects. RDA analysis demonstrated that *Akkermansia* negatively correlated with body weight and FBG level (Fig. 3I). These results indicate that HON effectively modulates gut microbiota dysbiosis in DM mice.

3.4. AKK alleviates diabetes in DM mice

Based on the 16S rRNA gene sequencing results showing HON treatment significantly enriched the genus *Akkermansia*, and given that AKK is the sole cultured species of the genus *Akkermansia*, we quantified AKK's relative abundance in fecal samples using qPCR [39]. The analysis revealed a 1300-fold increase in AKK levels following HON treatment in DM mice (Fig. 4A). The FMT experiment demonstrated elevated AKK abundance in receptor mice compared to DM-FMT mice (Fig. 4B). To evaluate HON's effect on AKK growth, we examined their interaction *in vitro* under anaerobic conditions. The results indicated that direct HON incubation did not promote AKK growth (Fig. S4A). However, when culturing fecal microbiota with varying HON concentrations *in vitro* and quantifying AKK abundance over time, we observed that HON promoted AKK growth in both dose- and time-dependent patterns (Fig. 4C).

Given that host mucin is essential for AKK survival and growth, we investigated HON's impact on mucin secretion and mucin-producing gene expression [40]. HON treatment significantly upregulated the mRNA expression of mucin-producing genes, including *Muc2*, *Muc3*, and *Muc4* (Fig. 4D). Alcian blue staining revealed increased mucin secretion in the colon following HON treatment (Fig. 4E). These observations suggest that HON facilitates AKK growth by enhancing mucin production in the intestinal lumen.

To elucidate AKK's role in diabetes alleviation, we administered live AKK or vehicle (PBS) to HFD-STZ-induced DM mice *via* oral gavage for 8 weeks (Fig. S4B). As demonstrated in Fig. 4F, AKK colonization was confirmed in DM mice. Consistent with HON intervention, AKK supplementation resulted in reduced body weight, FBG, and food and water consumption compared to non-supplemented mice (Figs. S4C–S4F). ITT, OGTT, and insulin results demonstrated AKK's ability to improve insulin resistance (Figs. S4G–S4K). Additionally, AKK intervention reversed the elevated epididymal fat index and liver index in DM mice while improving lipid metabolism (Figs. S4L–S4O). Furthermore, AKK inhibited damage to epididymal fat, liver, and pancreas, protected intestinal mucosa, and reduced endotoxin production (Figs. S4P and S4Q). These results confirm AKK's protective effects against diabetes.

3.5. HON enriches microbial TRP metabolites in DM mice

AKK is associated with the metabolism of short-chain fatty acids [41], TRP [42], and bile acids [43]. Recent studies have increasingly demonstrated connections between the metabolome and the molecular pathophysiology of DM [1]. To investigate whether HON improves diabetes through the bacteria-metabolite axis, an untargeted metabolomics study was conducted on feces and serum samples using UPLC-QTOF/MS. The PCA analysis revealed distinct metabolite profiles among the CON, DM, and HON groups in both feces and serum samples (Figs. 5A and S5A), suggesting that STZ-HFD and HON treatment significantly affected the metabolomic profiles. Differential metabolites were identified by comparing mass spectrograms and online databases using VIP > 1 and $P < 0.05$ (Figs. 5B and S5B). In feces samples, HFD-STZ treatment significantly altered 82 metabolites, while HON administration regulated 84 metabolites (Tables S6 and S7). Notably, HON intervention significantly reversed the concentration of 21 metabolites, with 9 upregulated and 12 down-regulated (Fig. 5C). In serum, HFD-STZ treatment modified 21 metabolites compared with CON mice, and HON intervention altered 34 metabolites compared with DM animals (Tables S8 and S9). HON administration reversed changes in 16 metabolites induced by HFD-STZ, with 6 upregulated and 10 down-regulated (Fig. S5C).

MetaboAnalyst 4.0 was used to analyze metabolic pathway alterations influenced by HON treatment. In fecal samples, the HFD-STZ model primarily affected pathways related to D-glutamine and D-glutamate metabolism, tryptophan (TRP) metabolism,

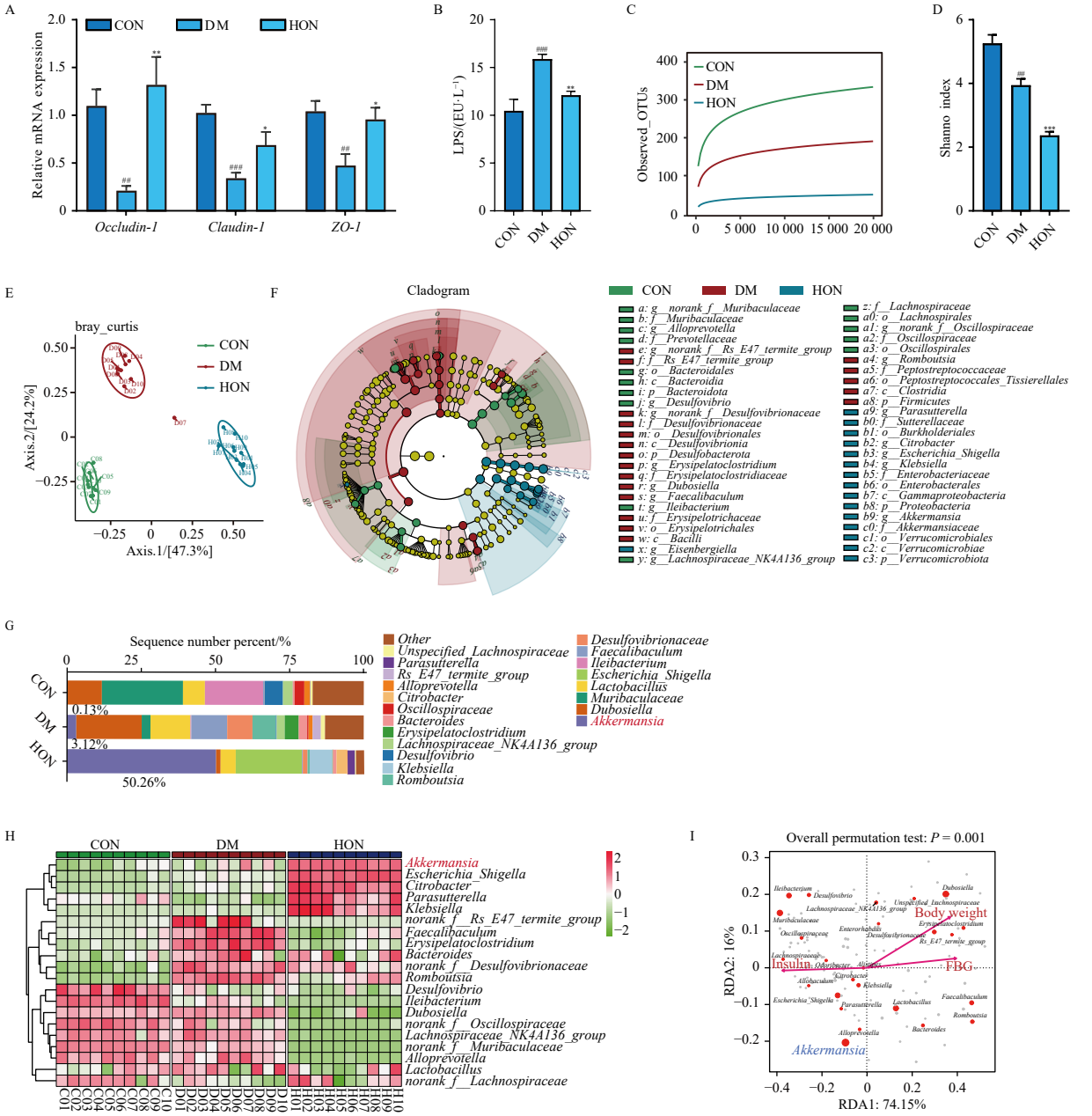

Fig. 3 HON ameliorates gut microbiota dysbiosis of DM mice. (A) Colon tissue relative mRNA abundance of *Occludin-1*, *Claudin-1*, and *ZO-1* (n = 8). The composition of fecal microbiota in mice from various groups was analyzed utilizing 16S rRNA gene sequencing. (B) LPS levels in serum (n = 7). (C and D) Rarefaction curves and Shannon diversity of gut microbiota among different groups (n = 10). (E) Weighted UniFrac PCoA analysis (n = 10). (F) A cladogram was obtained from LEfSe analysis (LDA > 4, n = 10). (G) Genus-level bacterial taxonomic profiling (n = 10). (H) Heat map: top 20 genus genera among CON, DM, and HON groups (n = 10). (I) RDA analysis between bacterial genus abundance and DM-associated symptoms (n = 10). Data were presented as mean ± SEM. $^{\#}P < 0.05$, $^{\#\#}P < 0.01$, $^{\#\#\#}P < 0.001$ *vs* CON group; $^{*}P < 0.05$, $^{**}P < 0.01$, and $^{***}P < 0.001$ *vs* DM group; NS, no significance.

and the biosynthesis of phenylalanine, tyrosine, and tryptophan. In contrast, HON intervention notably modulated TRP metabolism, aminoacyl-tRNA biosynthesis, and arginine and proline metabolism (Fig. 5D). Serum analysis similarly revealed that HON intervention predominantly influenced TRP metabolism (Fig. S5D). These findings indicate that TRP metabolism may be a key mechanism underlying HON's protective effects against diabetes.

Targeted quantification of TRP and its metabolites in feces was subsequently performed using UHPLC-QQQ/MS. TRP is metabolized in the gastrointestinal tract through three primary pathways: 1) the serotonin pathway, producing 5-HTP; 2) the KYN pathway, generating KYN and its downstream metabolites; and 3) direct microbial transformation of TRP into AHR ligands [44]. Compared with the CON group, fecal 5-HTP increased in DM mice, and the ratio of KYN to TRP increased in the serum of the DM group, but HON treatment did not reverse these elevations (Figs. S5E–S5H). Regarding fecal AHR agonists (I3C, IAA, IPA, and TA), HFD-STZ treatment decreased the concentration of IPA, TA, and total AHR agonists, while HON intervention increased the content of TA, I3C, and total AHR agonists (Fig. 5E). For serum AHR agonists, HFD-STZ treatment decreased the concentration of IAA, IPA, and total AHR agonists, while HON intervention increased the content of I3C and total AHR agonists (Fig. 5F). These results suggest that HON may improve diabetes through regulation of TRP metabolism.

3.6. TA produced by AKK attenuates the symptoms of DM mice

To examine whether TRP promotes AKK growth, different concentrations of TRP were added to the BHI-modified medium. The results demonstrated that TRP did not affect AKK growth *in vitro* (Fig. 6A). Further investigation involved incubating fecal mi-

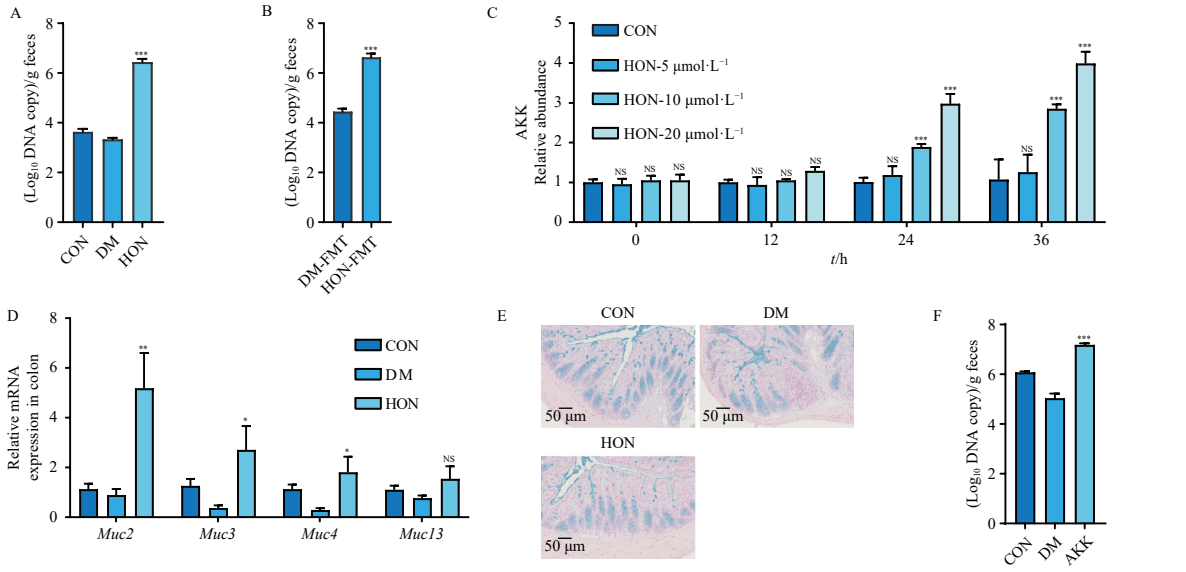

Fig. 4 The protective effects of AKK on DM mice. (A) Quantification of AKK in feces of CON, DM, and HON groups (n = 6). (B) Quantification of AKK in feces of DM-FMT and HON-FMT groups (n = 6). (C) Effect of HON on the relative abundance of AKK in fecal microbiota (n = 3), $^{***}P < 0.001$ *vs* CON group of corresponding time; NS, no significance. (D) Relative mRNA levels of mucin-generating genes in the colon (n = 8). (E) The colon with alcian blue staining (n = 3; scale bar, 50 μm). (F) Quantification of AKK in feces of CON, DM, and AKK groups (n = 6). Data were presented as mean ± SEM. $^{\#}P < 0.05$, $^{\#\#}P < 0.01$, $^{\#\#\#}P < 0.001$ *vs* CON group; $^{*}P < 0.05$, $^{**}P < 0.01$, and $^{***}P < 0.001$ *vs* DM group or DM-FMT group; NS, no significance.

crobiota with TRP for 36 h. Compared to the CON group, TRP supplementation enhanced the growth and reproduction of AKK (Fig. 6B). To evaluate AKK's ability to metabolize TRP, an *in vitro* culture system quantified the TRP metabolites. The analysis revealed that AKK metabolized TRP to produce 5-HTP, TA, I3C, and IAA (Fig. 6C).

Following untargeted and targeted metabolomics analysis revealing HON's ability to elevate TRP microbiota metabolite TA levels, and AKK's capacity to metabolize TRP into TA, subsequent investigation focused on whether TA intervention improves DM mice symptoms (Fig. 6D). Compared to the DM group, TA-treated mice demonstrated decreased weight gain, FBG levels, food consumption, and water consumption, while showing increased insulin levels (Figs. 6E–6I). TA treatment effectively improved blood glucose, insulin dysmetabolism, and lipid metabolism dysfunction in diabetic mice, as demonstrated by OGTT, ITT, organ index, blood lipids, and histomorphology of pancreatic, hepatic, and epididymal adipose tissues (Figs. 6J, 6K, and S6A–S6E). Additionally, TA treatment enhanced the intestinal barrier (Figs. 6L–6N). Western blotting and qPCR results indicated that TA supplementation activated the AHR signaling pathway (Figs. 6O and 6P). These results suggest that TA may improve diabetes through AHR pathway activation.

3.7. HON activates the AHR pathway to improve diabetes

Given that HON's beneficial effects were associated with changes in intestinal microbiota, TRP metabolism, and AHR activation, subsequent investigation focused on the AHR pathway's involvement in HON's protective effects, which can be activated by bacterial-produced TRP metabolites. The results demonstrated that HON treatment elevated the mRNA expression of *Ahr* and *Cyp1a1*, target gene of AHR activation in the colon (Fig. 7A). Western blotting analysis confirmed that HON administration increased the protein expressions of AHR and CYP1A1 (Fig. 7B). As AKK and AHR activation enhance colon anti-microbial peptide production and strengthen the intestinal barrier [39, 45], examination of relative mRNA expression of anti-microbial peptides in the colon revealed that HON supplementation increased the expression of *Tff3* and *Reg3g* compared with the DM group (Fig. S7A). Additionally, analysis of mRNA and protein expression of AHR-related target genes in diabetic mice after AKK intervention showed that AKK administration increased the mRNA expression of *Ahr*, *Cyp1a1*, *Reg3g*, and *Reg3b* (Fig. S7B), and the protein expression of AHR and CYP1A1.

To investigate the physiological significance of AHR activity, CH223191, an AHR antagonist, was employed to validate HON's impact on AHR activation in diabetic mice (Fig. 7C). While HON maintained improvements in body weight, FBG, food, and water consumption after AHR inhibition, these effects were attenuated by cotreatment with CH2223191 (Figs. 7D–7G). CH223191 also diminished HON's beneficial effects on glucose and insulin dysmetabolism in diabetic mice, as evidenced by OGTT, ITT, and pancreatic tissue histomorphology (Figs. 7H–7L). Furthermore, CH223191 + HON-treated mice exhibited less improvement in lipid metabolism dysfunction compared to HON treatment alone (Figs. S7D–S7H), and HON's effect on the intestinal barrier was negated by CH223191 treatment (Figs. 7M and 7N). HON treatment increased intestinal expression of *Ahr*, *Cyp1a1*, *interleukin (Il)*-22, *Reg3g*, and *Reg3b*, but cotreatment with CH223191 inhibited HON-induced AHR activation (Fig. S7I). Western blotting analysis confirmed that CH223191 intervention inhibited HON's effect on AHR activation (Fig. 7O). These results suggest that AHR pathways partially mediate HON's therapeutic effects against diabetes.

3.8. HON induces the secretion of the incretin hormone GLP-1 by activating AHR

Previous research has demonstrated AKK's ability to stimulate GLP-1 secretion [46]. The present data showed that AKK intervention increased serum total GLP-1 levels in diabetic mice (Fig. 8A) and elevated the mRNA level (Fig. 8B, P = 0.16) of intestinal proglucagon, which was subsequently confirmed by Western blotting analysis (Fig. 8C). These findings suggest that HON's protective effect is associated with AKK-mediated GLP-1 modulation.

Microbiota-derived AHR agonists effectively stimulate the incretin hormone GLP-1 [47]. In DM mice, TA elevated serum GLP-1 levels (Fig. 8D). Western blotting and qPCR analyses revealed that changes in intestinal GLP-1 expression corresponded with alterations in serum GLP-1 levels (Figs. 8E and 8F). HON increased both intestinal *Gcg* mRNA expression and total serum GLP-1

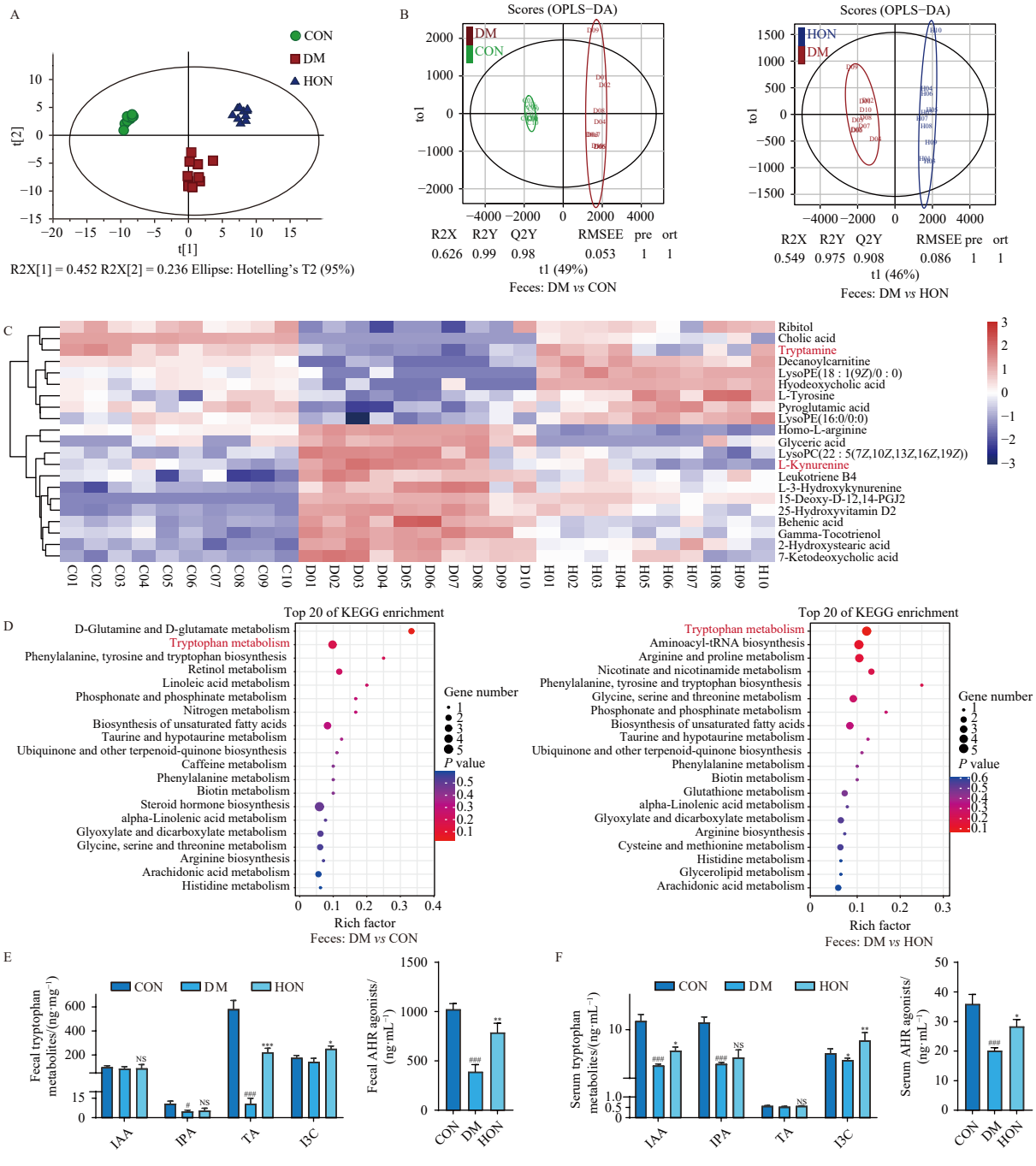

Fig. 5 HON enriches TRP metabolites in DM mice. (A) PCA score plots were conducted to distinguish the fecal metabolome from CON, DM, and HON groups (n = 10). (B) The OPLS-DA scores plot discriminated fecal metabolites in DM *vs* CON mice, and the OPLS-DA scores plot discriminated fecal metabolites in DM *vs* HON mice (n = 10). (C) Differential metabolites changed by HFD-STZ and reversed by HON (n = 10). (D) Pathways were significantly influenced by HFD-STZ (left) or HON (right) in fecal samples. (E) The effect of HON on TRP metabolites (IAA, IPA, TA, I3C, and total AHR agonists) in feces (n = 8). (F) The effect of HON on TRP metabolites (IAA, IPA, TA, I3C, and total AHR agonists) in serum (n = 8). Data were presented as mean ± SEM. $^{\#}P < 0.05$, $^{\#\#}P < 0.01$, $^{\#\#\#}P < 0.001$ *vs* CON group; $^{*}P < 0.05$, $^{**}P < 0.01$, and $^{***}P < 0.001$ *vs* DM group; NS, no significance.

levels in DM mice, though these effects were nullified by CH223191 cotreatment (Figs. 8G and 8H). Western blotting analysis confirmed these findings (Fig. 8I). Subsequently, we examined HON's direct effect on GLP-1 secretion in STC-1 cells. We confirmed AHR expression in STC-1 cells and its inhibition by CH223191 (Figs. S8A and S8B). ELISA results showed that HON did not enhance GLP-1 secretion in PA-induced STC-1 cells (Fig. 8J). While TA treatment increased GLP-1 secretion in STC-1 cells, this beneficial effect was eliminated by CH223191 cotreatment (Figs. 8K, 8L, and S8C). These results suggest that HON's stimulatory effect on GLP-1 secretion depends on AHR activation by TRP metabolites.

4. Discussion

This investigation revealed the essential role of AKK and TA in mediating HON's anti-diabetic effects through fecal transplantation, antibiotic experiments, untargeted/targeted metabolomics, and pharmacological studies. The findings demonstrated that HON's anti-diabetic efficacy depends on gut microbiota composition. HON showed no significant effects or adverse reactions on blood glucose and lipid metabolism in normal mice, indicating its potential as a safe and promising therapeutic agent for diabetes treatment (Fig. S10). Significantly, HON enriched AKK 1300-fold in diabetic mice feces, and AKK intervention produced anti-dia-

betic effects comparable to HON treatment. Furthermore, HON enhanced the production of TRP bacterial metabolites, particularly TA. AKK effectively converted TRP into TA and other metabolites *in vitro*. Notably, TA demonstrated substantial anti-diabetic effects in DM mice. Moreover, HON, AKK, and TA activated AHR to enhance GLP-1 production. AHR receptor inhibition eliminated both the therapeutic effects against diabetes and the HON-induced increase in GLP-1 secretion. Collectively, these findings demonstrate HON's significant therapeutic effect on diabetes through AKK regulation and TRP metabolite modulation.

Multiple studies have demonstrated the pharmacological activities of polyphenols with low bioavailability, such as resveratrol [48] and curcumin [49], which achieve their effects through gut microbiota modulation. The gut microbiota, which plays a crucial role in the development of DM, interacts with the host both directly and indirectly through bacterial metabolites, includ-

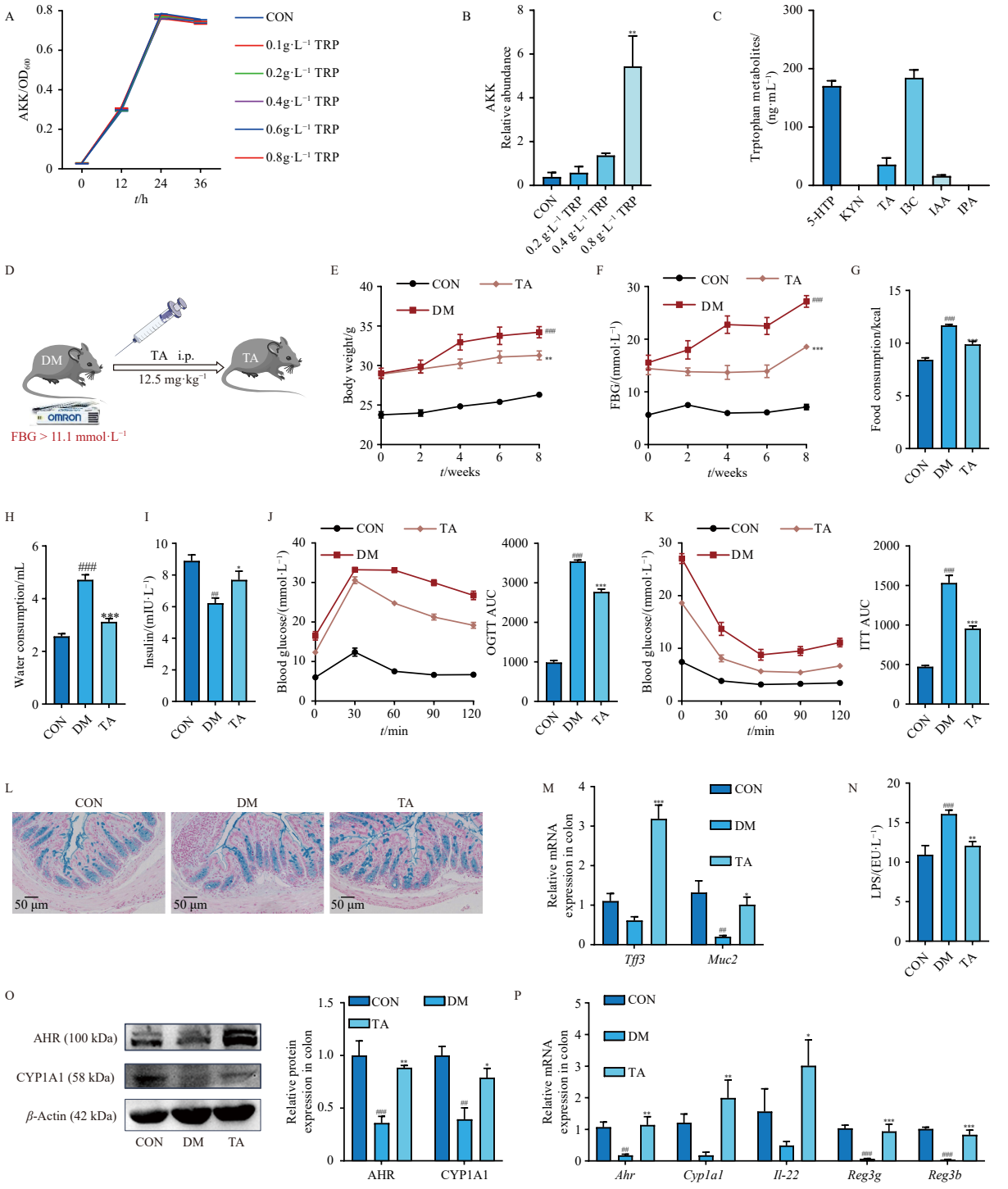

Fig. 6 TA produced by AKK attenuates the symptoms of DM mice. (A) The growth curve of AKK with different concentrations of tryptophan (n = 3). (B) The effect of tryptophan on the relative abundance of AKK in fecal microbiota (n = 3), $^{**}P$ < 0.01 *vs* CON group. (C) The concentrations of tryptophan metabolites in the supernatant of AKK (n = 3). (D) Study design of TA intervention (n = 8). (E) Body weight, (F) FBG, (G) food consumption, (H) water consumption, and (I) levels of insulin. (J) Blood glucose levels in OGTT with AUC. (K) Blood glucose levels in ITT with AUC. (L) The colon with alcian blue staining (n = 3; scale bar, 50 μm). (M) The relative mRNA expression of *Tff3*, and *Muc2*. (N) Levels of LPS. (O) Western blotting of the AHR and CYP1A1 protein expression in the colon (n = 3). (P) The relative mRNA expression of target genes (*Ahr*, *Cyp1a1*, *Il-22*, *Reg3g*, and *Reg3b*, n = 8). Data were presented as mean ± SEM. $^{\#}P$ < 0.05, $^{\#\#}P$ < 0.01, $^{\#\#\#}P$ < 0.001 *vs* CON group; $^{*}P$ < 0.05, $^{**}P$ < 0.01, and $^{***}P$ < 0.001 *vs* DM group; NS, no significance.

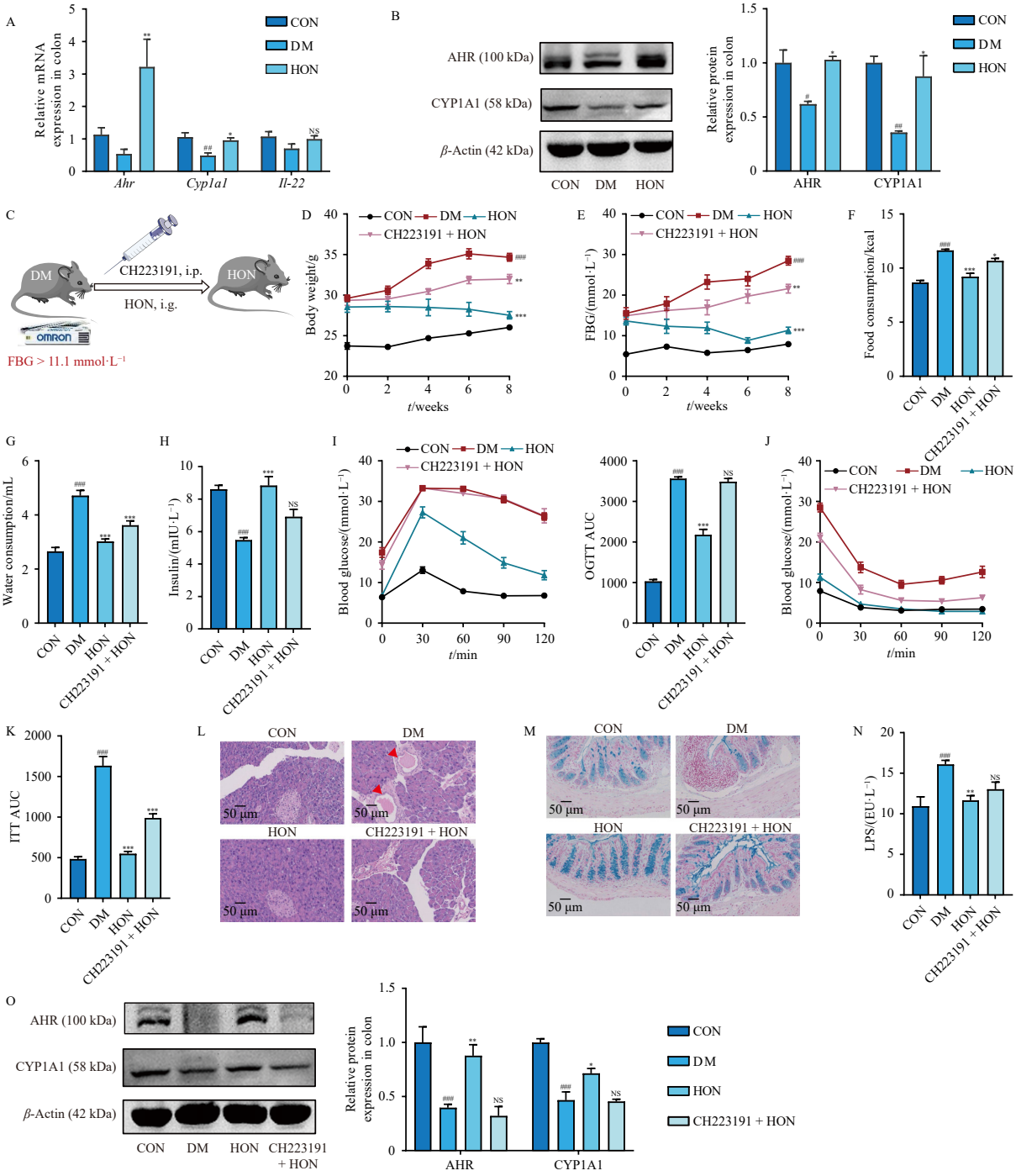

Fig. 7 HON activates the AHR pathway to improve DM in mice. (A) The relative mRNA expression of target genes (*Ahr*, *Cyp1a1*, and *Il-22*, $n = 8$). (B) Western blotting of the AHR and CYP1A1 protein expression in the colon ($n = 3$). (C) Study design of CH223191 intervention ($n = 8$). (D) Body weight. (E) FBG. (F) Food consumption. (G) Water consumption. (H) Levels of insulin. (I) Blood glucose levels in OGTT with AUC. (J and K) Blood glucose levels in ITT with AUC. (L) H&E staining of the pancreatic tissue ($n = 3$; scale bar, 50 μm). (M) The colon with alcian blue staining ($n = 3$; scale bar, 50 μm). (N) The concentration of LPS. (O) Western blotting of the AHR and CYP1A1 protein expression in the colon ($n = 3$). Data were presented as mean ± SEM. $^{\#}P < 0.05$, $^{\#\#}P < 0.01$, $^{\#\#\#}P < 0.001$ *vs* CON group; $^{*}P < 0.05$, $^{**}P < 0.01$, and $^{***}P < 0.001$ *vs* DM group; NS, no significance.

ing saturated short-chain fatty acids [50], bile acids [51], and TRP [47]. Although the oral bioavailability of HON is approximately 5%, HON supplementation significantly attenuates hyperglycemia, insulin resistance, and lipid metabolism disorder in DM mice. This suggests that HON may exert its anti-diabetic effect through modulation of gut microbiota.

DM can compromise intestinal integrity, as evidenced by reduced levels of anti-microbial peptides, decreased mucus layer thickness, and insufficient tight junction proteins [52]. Similar results were observed in this study, with HON supplementation demonstrating improvement in these symptoms. Probiotics are established modulators of gut microbiota that prevent DM [53]. Using 16s rRNA gene sequencing to identify key bacterial changes induced by HON, this study demonstrates that HON induces a significant increase (1300-fold) in the abundance of AKK, a probiotic known to improve insulin resistance [39]. Direct incubation with HON did not promote AKK growth. While previous studies have shown that polyphenols can enhance AKK abundance, the precise mechanism remains unclear [54]. Dong et al. demonstrated that berberine indirectly promotes AKK growth by stimulating gut mucin secretion [40]. The present findings suggest that HON may enhance AKK abundance through similar mechanisms. Addition-

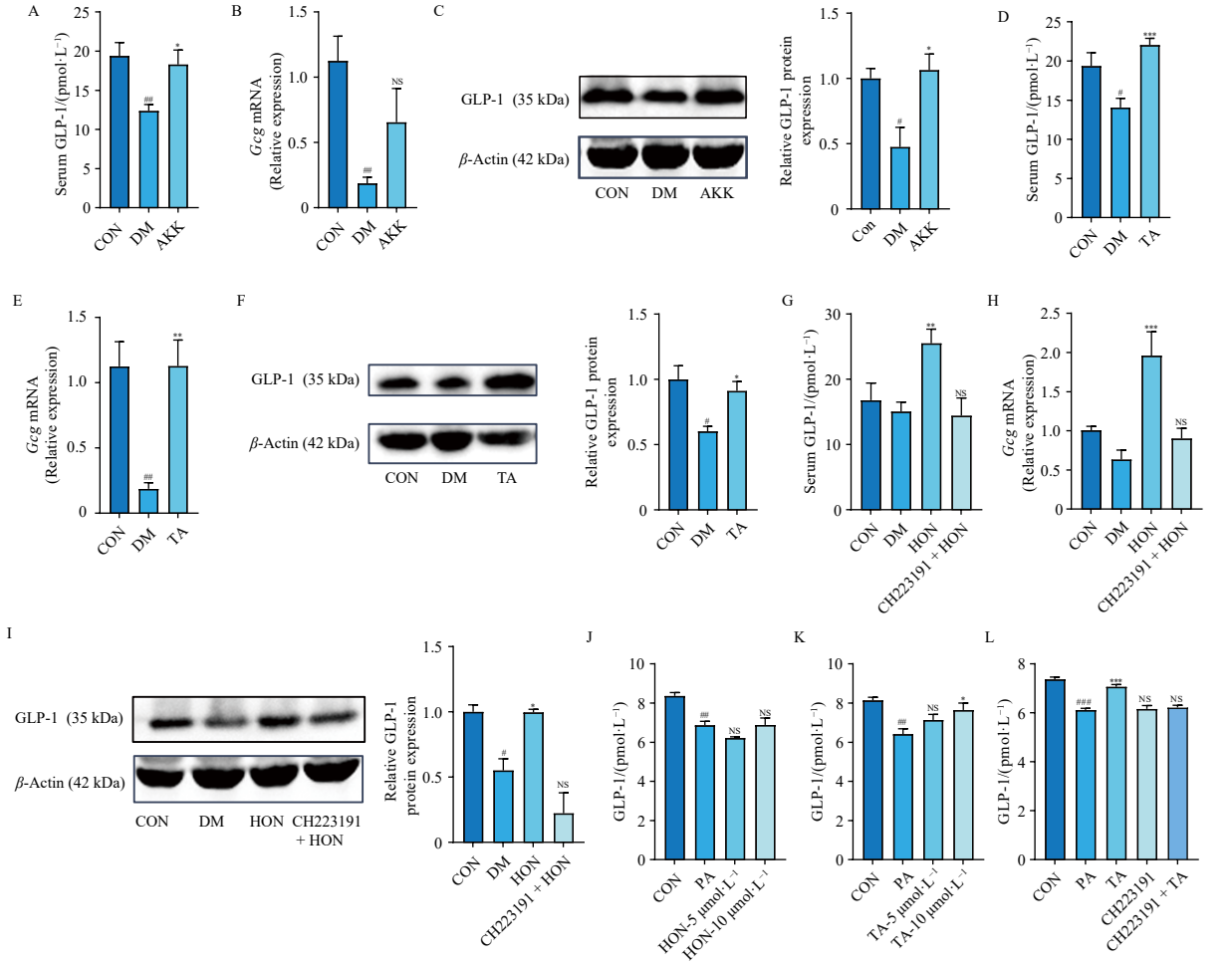

Fig. 8 HON induces the secretion of the incretin hormone GLP-1 by activating AHR. (A and B) The serum GLP-1 levels and relative mRNA expression of *Gcg* in the colon after AKK treatment (n = 8). (C) Western blotting of the GLP-1 protein expression in the colon after AKK treatment (n = 3). (D and E) The serum GLP-1 levels and relative mRNA expression of *Gcg* in the colon after TA treatment (n = 8). (F) Western blotting of the GLP-1protein expression in the colon after TA treatment (n = 3). (G and H) The relative serum GLP-1 levels and mRNA expression of *Gcg* in the colon after CH223191 treatment (n = 8). (I) Western blotting of the GLP-1 protein expression in the colon after CH223191 treatment (n = 3). (J) Effect of HON on GLP-1 secretion induced by PA in STC-1 cells (n = 3). (K) Effect of TA on GLP-1 secretion induced by PA in STC-1 cells (n = 3). (L) Effect of TA on GLP-1 secretion induced by PA in STC-1 cells after CH223191 administration (n = 3). Data were presented as mean ± SEM. $^{\#}P < 0.05$, $^{\#\#}P < 0.01$, $^{\#\#\#}P < 0.001$ *vs* CON group; $^{*}P < 0.05$, $^{**}P < 0.01$, and $^{***}P < 0.001$ *vs* DM group or PA group; NS, no significance.

ally, AKK intervention demonstrated significant improvements in diabetes-related symptoms in diabetic mice.

To elucidate the mechanisms by which HON-induced modifications of the intestinal microbiota reduce diabetes, analyses of serum and fecal metabolites identified the critical role of TRP metabolism in HON's protective effect against diabetes. Targeted metabolome analysis revealed that HON increased the levels of TRP microbial metabolites TA, I3C, and total AHR agonists. Various microorganisms contribute to TRP metabolism in the gut. Administration of *Lactobacillus reuteri* increases indole-3-lactic acid levels, thereby suppressing colorectal tumorigenesis [55]. *Bifidobacterium longum* CCFM1029 upregulates TRP metabolites I3C to activate AHR-mediated immune response and alleviate atopic dermatitis symptoms [32]. The data revealed that AKK metabolizes TRP into 5-HTP, TA, and I3C *in vitro*. A significant increase in I3C and TA levels was observed in the feces of diabetic mice following HON treatment. Given the substantial increase in TA observed in both untargeted and targeted metabolomics analyses, its impact on diabetes was investigated. TA, converted from TRP by *Clostridium sporogenes* and *Ruminococcus gnavus* [56], reduces pro-inflammatory cytokine production in macrophages stimulated by fatty acids and LPS [57]. The elevated TA levels in HON-treated DM mice feces, combined with AKK's ability to metabolize TRP into TA, led to the investigation of TA's potential to ameliorate diabetes symptoms in HFD-STZ-induced mice. The data indicate that TA exhibits similar therapeutic effects as HON in DM mice. TA inhibits glucose-induced hyperglycemia and enhances glucose-elicited insulin release [58]. However, a recent study contradicts these findings, suggesting that TA may impair insulin sensitivity [59]. This discrepancy may result from variations in disease models and requires additional investigation.

Both humans and rats with metabolic syndrome demonstrate impaired AHR agonist activity, and treatment with AHR agonist Ficz or AHR ligand-producing bacteria *Lactobacillus* strain improves metabolic disorders [47]. This study demonstrates that HON's enhancement of mucus and anti-microbial peptide production correlates with restored AHR-related gene expression, including *Il-22*, *Cyp1a1*, and *Ahr*. Conversely, reduced levels of *Reg3b*, *Reg3g*, and mucus production correspond with decreased levels of *Il-22*, *Cyp1a1*, and A*hr*. To examine AHR's direct involvement in HON's effects, DM mice were treated with AHR antagonist CH223191. The antagonist nullified HON's beneficial effects, indicating that AHR activation is essential for HON's therapeutic effect on diabetes.

The incretin hormone GLP-1 plays a crucial role in regulating glucose metabolism. Drugs that mimic GLP-1 actions are widely used in treating DM [60]. AKK and microbiota-derived AHR agonists have demonstrated the ability to induce GLP-1 secretion [46, 47]. However, previous studies focused solely on serum GLP-1 secretion. This study investigated HON's impact on GLP-1 secretion in DM mice and PA-induced STC-1 cells. The findings demonstrated that HON, AKK, and TA induced serum GLP-1 secretion and elev-

ated intestinal protein expression. However, in PA-induced STC-1 cells, HON did not promote GLP-1 secretion. While TA treatment increased GLP-1 secretion in STC-1 cells, this effect was neutralized by the AHR inhibitor CH223191. These results indicate that HON's effect on GLP-1 enhancement relies on AHR activation by TRP metabolites. This suggests that screening GLP-1 agents from AHR agonists may represent a promising strategy for diabetes drug discovery.

Overall, the results revealed a distinct mechanism whereby HON's protective benefits in diabetic mice may be mediated through AKK and microbiota-dependent AHR signaling. BHI medium was selected to study HON's effect on AKK proliferation in fecal microbiota, as it supports AKK bacterial growth. However, research indicates that medium type and culture duration can influence human gut microbiome growth [61]. While a control group was established to account for these effects, future studies should further examine both medium type and culture duration. A limitation of this study was the lack of consideration for other gut microbes' potential contribution to TRP metabolism. Future research will investigate the effects of HON and AKK using a germ-free mouse model and AHR knockout mice to determine the gut microbiota's role and its TRP metabolism.

5. Conclusion

In summary, this study demonstrates that HON improves glycolipid metabolism in HFD-STZ-induced diabetic mice. The mechanism likely operates through enriching AKK and regulating TRP metabolism to activate AHR and enhance GLP-1 production. Significantly, both AKK and the TRP metabolite TA showed potential in improving diabetes symptoms. This study elucidates a novel mechanism underlying HON's beneficial effects against diabetes, suggesting that supplementation with TRP microbial metabolites to activate AHR receptors may constitute a novel therapeutic approach for diabetes.

Funding

This study was supported by the National Key Research and Development Program of China (No. 2023YFC3502605), the National Natural Science Foundation of China (Nos. 82104360, 82274074, and 82204598), Jiangsu Funding Program for Excellent Postdoctoral Talent, and China Postdoctoral Science Foundation (No. 2022M713483).

Data availability

OTU tables of the gut microbiome and UPLC-QTOF/MS metabolomics data are included in supplementary materials. All 16S rRNA gene sequencing reads data have beendeposited in NCBI Sequence Read Archive (PRJNA994056).

Declaration of competing interest

The authors declare no conflicts of interest.

References

1 Li X, Watanabe K, Kimura I. Gut microbiota dysbiosis drives and implies novel therapeutic strategies for diabetes mellitus and related metabolic diseases. *Front Immunol*. 2017;8:1882. https://doi.org/10.3389/fimmu.2017.01882.
2 Jia W, Panagiotou G. Recent advances in diabetes and microbiota. *Sci Bull*. 2022;67(17):1720-1723. https://doi.org/10.1016/j.scib.2022.07.027.
3 Zhou W, Yang T, Xu W, et al. The polysaccharides from the fruits of *Lycium barbarum* L. confer anti-diabetic effect by regulating gut microbiota and intestinal barrier. *Carbohydr Polym*. 2022;291:119626. https://doi.org/10.1016/j.carbpol.2022.119626.
4 Amiel SA, Frier BM, Heller SR, et al. Hypoglycaemia, cardiovascular disease, and mortality in diabetes: epidemiology, pathogenesis, and management. *Lancet Diabetes Endocrinol*. 2019;7(5):385-396. https://doi.org/10.1016/S2213-8587(18)30315-2.
5 Canfora EE, Meex RCR, Venema K, et al. Gut microbial metabolites in obesity, NAFLD and T2DM. *Nat Rev Endocrinol*. 2019;15(5):261-273. https://doi.org/10.1038/s41574-019-0156-z.
6 Huang S, Shao L, Chen M, et al. Biotransformation differences of ginsenoside compound K mediated by the gut microbiota from diabetic patients and healthy subjects. *Chin J Nat Med*. 2023;21(10):723-729. https://doi.org/10.1016/S1875-5364(23)60402-9.
7 Crudele L, Gadaleta RM, Cariello M, et al. Gut microbiota in the pathogenesis and therapeutic approaches of diabetes. *EBioMedicine*. 2023;97:104821. https://doi.org/10.1016/j.ebiom.2023.104821.
8 Zhang Y, Liu L, Wei C, et al. Vitamin K2 supplementation improves impaired glycemic homeostasis and insulin sensitivity for type 2 diabetes through gut microbiome and fecal metabolites. *BMC Med*. 2023;21(1):174. https://doi.org/10.1186/s12916-023-02880-0.
9 Vallianou NG, Stratigou T, Tsagarakis S. Microbiome and diabetes: where are we now? *Diabetes Res Clin Pract*. 2018;146:111-118. https://doi.org/10.1016/j.diabres.2018.10.008.
10 Yang X, Wang Z, Niu J, et al. Pathobionts from chemically disrupted gut microbiota induce insulin-dependent diabetes in mice. *Microbiome*. 2023;11:62. https://doi.org/10.1186/s40168-023-01507-z.
11 Wu H, Esteve E, Tremaroli V, et al. Metformin alters the gut microbiome of individuals with treatment-naive type 2 diabetes, contributing to the therapeutic effects of the drug. *Nat Med*. 2017;23(7):850-858. https://doi.org/10.1038/nm.4345.
12 Zhang Y, Hu J, Tan H, et al. *Akkermansia muciniphila*, an important link between dietary fiber and host health. *Curr Opin Food Sci*. 2022;47:100905. https://doi.org/10.1016/j.cofs.2022.100905.
13 Zhang Y, Yang Y, Ding L, et al. Emerging applications of metabolomics to assess the efficacy of traditional Chinese medicines for treating type 2 diabetes mellitus. *Front Pharmacol*. 2021;12:735410. https://doi.org/10.3389/fphar.2021.735410.
14 Fan Y, Pedersen O. Gut microbiota in human metabolic health and disease. *Nat Rev Microbiol*. 2021;19(1):55-71. https://doi.org/10.1038/s41579-020-0433-9.
15 Liu Z, Dai X, Zhang H, et al. Gut microbiota mediates intermittent-fasting alleviation of diabetes-induced cognitive impairment. *Nat Commun*. 2020;11(1):855. https://doi.org/10.1038/s41467-020-14676-4.
16 Giannoudaki E, Hernandez-Santana YE, Mulfaul K, et al. Interleukin-36 cytokines alter the intestinal microbiome and can protect against obesity and metabolic dysfunction. *Nat Commun*. 2019;10(1):4003. https://doi.org/10.1038/s41467-019-11944-w.
17 Bui D, Li L, Yin T, et al. Pharmacokinetic and metabolic profiling of key active components of dietary supplement *Magnolia officinalis* extract for prevention against oral carcinoma. *J Agric Food Chem*. 2020;68(24):6576-6587. https://doi.org/10.1021/acs.jafc.0c01475.
18 Pillai VB, Samant S, Sundaresan NR, et al. Honokiol blocks and reverses cardiac hypertrophy in mice by activating mitochondrial Sirt3. *Nat Commun*. 2015;6:6656. https://doi.org/10.1038/ncomms7656.
19 Cho JH, Jeon YJ, Park SM, et al. Multifunctional effects of honokiol as an anti-inflammatory and anti-cancer drug in human oral squamous cancer cells and xenograft. *Biomaterials*. 2015;53:274-284. https://doi.org/10.1016/j.biomaterials.2015.02.091.
20 Sun J, Wang Y, Fu X, et al. *Magnolia officinalis* extract contains potent inhibitors against PTP1B and attenuates hyperglycemia in *db/db* mice. *Biomed Res Int*. 2015;2015:139451. https://doi.org/10.1155/2015/139451.
21 Kerr M, Miller JJ, Thapa D, et al. Rescue of myocardial energetic dysfunction in diabetes through the correction of mitochondrial hyperacetylation by honokiol. *JCI Insight*. 2020;5(17):e140326. https://doi.org/10.1172/jci.insight.140326.
22 Li CG, Ni CL, Yang M, et al. Honokiol protects pancreatic beta cell against high glucose and intermittent hypoxia-induced injury by activating Nrf2/ARE pathway *in vitro* and *in vivo*. *Biomed Pharmacother*. 2018;97:1229-1237. https://doi.org/10.1016/j.biopha.2017.11.063.
23 Yang J, Shang J, Yang L, et al. Nanotechnology-based drug delivery systems for honokiol: enhancing therapeutic potential and overcoming limitations. *Int J Nanomed*. 2023;18:6639-6665. https://doi.org/10.2147/IJN.S431409.
24 Peng D, Tian W, An M, et al. Characterization of antidiabetic effects of *Dendrobium officinale* derivatives in a mouse model of type 2 diabetes mellitus. *Food Chem*. 2023;399:133974. https://doi.org/10.1016/j.foodchem.2022.133974.
25 Hosomi K, Saito M, Park J, et al. Oral administration of *Blautia wexlerae* ameliorates obesity and type 2 diabetes *via* metabolic remodeling of the gut microbiota. *Nat Commun*. 2022;13(1):4477. https://doi.org/10.1038/s41467-022-32015-7.
26 Lin Y, Wang ZY, Wang MJ, et al. Baicalin attenuate diet-induced metabolic syndrome by improving abnormal metabolism and gut microbiota. *Eur J Pharmacol*. 2022;925:174996. https://doi.org/10.1016/j.ejphar.2022.174996.
27 Jiang ZM, Zeng SL, Huang TQ, et al. Sinomenine ameliorates rheumatoid arthritis by modulating tryptophan metabolism and activating aryl hydrocarbon receptor *via* gut microbiota regulation. *Sci Bull*. 2023;68(14):1540-1555. https://doi.org/10.1016/j.scib.2023.06.027.
28 Huang TQ, Chen YX, Zeng SL, et al. Bergenin alleviates ulcerative colitis by decreasing gut commensal *Bacteroides vulgatus*-mediated elevated branched-chain amino acids. *J Agric Food Chem*. 2024;72(7):3606-3621. https://doi.org/10.1021/acs.jafc.3c09448.
29 Jiang L, Hong Y, Xiao P, et al. The role of fecal microbiota in liver toxicity induced by perfluorooctane sulfonate in male and female mice. *Environ Health Perspect*. 2022;130(6):67009. https://doi.org/10.1289/EHP10281.
30 Gao B, Chi L, Tu P, et al. The carbamate aldicarb altered the gut microbiome,

metabolome, and lipidome of C57BL/6J mice. *Chem Res Toxicol*. 2019;32(1): 67-79. https://doi.org/10.1021/acs.chemrestox.8b00179.
31 Wang J, Zhou L, Lei H, et al. Simultaneous quantification of amino metabolites in multiple metabolic pathways using ultra-high performance liquid chromatography with tandem-mass spectrometry. *Sci Rep*. 2017;7: 1423. https://doi.org/10.1038/s41598-017-01435-7.
32 Fang Z, Pan T, Li L, et al. *Bifidobacterium longum* mediated tryptophan metabolism to improve atopic dermatitis *via* the gut-skin axis. *Gut Microbes*. 2022;14(1):2044723. https://doi.org/10.1080/19490976.2022.2044723.
33 Yin J, Song Y, Hu Y, et al. Dose-dependent beneficial effects of tryptophan and its derived metabolites on Akkermansia in vitro: a preliminary prospective study. *Microorganisms*. 2021;9(7):1511. https://doi.org/10.3390/microorganisms9071511.
34 Dopkins N, Becker W, Miranda K, et al. Tryptamine attenuates experimental multiple sclerosis through activation of Aryl hydrocarbon receptor. *Front Pharmacol*. 2021;11:619265. https://doi.org/10.3389/fphar.2020.619265.
35 Zhuang P, Li H, Jia W, et al. Eicosapentaenoic and docosahexaenoic acids attenuate hyperglycemia through the microbiome-gut-organs axis in *db/db* mice. *Microbiome*. 2021;9:185. https://doi.org/10.1186/s40168-021-01126-6.
36 Trabelsi MS, Daoudi M, Prawitt J, et al. Farnesoid X receptor inhibits glucagon-like peptide-1 production by enteroendocrine L cells. *Nat Commun*. 2015;6:7629. https://doi.org/10.1038/ncomms8629.
37 Zhang Y, Huang S, Li P, et al. Pancreatic cancer-derived exosomes suppress the production of GIP and GLP-1 from STC-1 cells *in vitro* by down-regulating the PCSK1/3. *Cancer Lett*. 2018;431:190-200. https://doi.org/10.1016/j.canlet.2018.05.027.
38 Liu J, Zhang D, Yang Z, et al. Wheat alkylresorcinols modulate glucose homeostasis through improving GLP-1 secretion in high-fat-diet-induced obese mice. *J Agric Food Chem*. 2023;71(43):16125-16136. https://doi.org/10.1021/acs.jafc.3c04664.
39 Everard A, Belzer C, Geurts L, et al. Cross-talk between *Akkermansia muciniphila* and intestinal epithelium controls diet-induced obesity. *Proc Natl Acad Sci U S A*. 2013;110(22):9066-9071. https://doi.org/10.1073/pnas.1219451110.
40 Dong C, Yu J, Yang Y, et al. Berberine, a potential prebiotic to indirectly promote *Akkermansia* growth through stimulating gut mucin secretion. *Biomed Pharmacother*. 2021;139:111595. https://doi.org/10.1016/j.biopha.2021.111595.
41 Liu MJ, Yang JY, Yan ZH, et al. Recent findings in *Akkermansia muciniphila*-regulated metabolism and its role in intestinal diseases. *Clin Nutr*. 2022;41 (10):2333-2344. https://doi.org/10.1016/j.clnu.2022.08.029.
42 Gu Z, Pei W, Shen Y, et al. *Akkermansia muciniphila* and its outer protein Amuc_1100 regulates tryptophan metabolism in colitis. *Food Funct*. 2021;12 (20):10184-10195. https://doi.org/10.1039/D1FO02172A.
43 Rao Y, Kuang Z, Li C, et al. Gut *Akkermansia muciniphila* ameliorates metabolic dysfunction-associated fatty liver disease by regulating the metabolism of L-aspartate *via* gut-liver axis. *Gut Microbes*. 2021;13(1):1-19. https://doi.org/10.1080/19490976.2021.1927633.
44 Agus A, Planchais J, Sokol H. Gut microbiota regulation of tryptophan metabolism in health and disease. *Cell Host Microbe*. 2018;23(6):716-724. https://doi.org/10.1016/j.chom.2018.05.003.
45 Wrzosek L, Ciocan D, Hugot C, et al. Microbiota tryptophan metabolism induces aryl hydrocarbon receptor activation and improves alcohol-induced liver injury. *Gut*. 2021;70(7):1299-1308. https://doi.org/10.1136/gutjnl-2020-321565.
46 Yoon HS, Cho CH, Yun MS, et al. *Akkermansia muciniphila* secretes a glucagon-like peptide-1-inducing protein that improves glucose homeostasis and ameliorates metabolic disease in mice. *Nat Microbiol*. 2021;6(5):563-573. https://doi.org/10.1038/s41564-021-00880-5.
47 Natividad JM, Agus A, Planchais J, et al. Impaired aryl hydrocarbon receptor ligand production by the gut microbiota is a key factor in metabolic syndrome. *Cell Metab*. 2018;28(5):737-49.e4. https://doi.org/10.1016/j.cmet.2018.07.001.
48 Chen M, Hou P, Zhou M, et al. Resveratrol attenuates high-fat diet-induced non-alcoholic steatohepatitis by maintaining gut barrier integrity and inhibiting gut inflammation through regulation of the endocannabinoid system. *Clin Nutr*. 2020;39(4):1264-1275. https://doi.org/10.1016/j.clnu.2019.05.020.
49 Li S, You J, Wang Z, et al. Curcumin alleviates high-fat diet-induced hepatic steatosis and obesity in association with modulation of gut microbiota in mice. *Food Res Int*. 2021;143:110270. https://doi.org/10.1016/j.foodres.2021.110270.
50 Zhao L, Zhang F, Ding X, et al. Gut bacteria selectively promoted by dietary fibers alleviate type 2 diabetes. *Science*. 2018;359(6380):1151-1156. https://doi.org/10.1126/science.aao5774.
51 Chen B, Bai Y, Tong F, et al. Glycoursodeoxycholic acid regulates bile acids level and alters gut microbiota and glycolipid metabolism to attenuate diabetes. *Gut Microbes*. 2023;15(1):2192155. https://doi.org/10.1080/19490976.2023.2192155.
52 Wang X, Yang Z, Xu X, et al. Odd-numbered agaro-oligosaccharides alleviate type 2 diabetes mellitus and related colonic microbiota dysbiosis in mice. *Carbohydr Polym*. 2020;240:116261. https://doi.org/10.1016/j.carbpol.2020.116261.
53 Wu TR, Lin CS, Chang CJ, et al. Gut commensal *Parabacteroides goldsteinii* plays a predominant role in the anti-obesity effects of polysaccharides isolated from Hirsutella sinensis. *Gut*. 2019;68(2):248-262. https://doi.org/10.1136/gutjnl-2017-315458.
54 Gao X, Yue C, Tian R, et al. The regulatory effects of specific polyphenols on *Akkermansia* are dependent on uridine. *Food Chem*. 2023;410:135367. https://doi.org/10.1016/j.foodchem.2022.135367.
55 Han JX, Tao ZH, Wang JL, et al. Microbiota-derived tryptophan catabolites mediate the chemopreventive effects of statins on colorectal cancer. *Nat Microbiol*. 2023;8(5):919-933. https://doi.org/10.1038/s41564-023-01363-5.
56 Williams BB, Van Benschoten AH, Cimermancic P, et al. Discovery and characterization of gut microbiota decarboxylases that can produce the neurotransmitter tryptamine. *Cell Host Microbe*. 2014;16(4):495-503. https://doi.org/10.1016/j.chom.2014.09.001.
57 Krishnan S, Ding Y, Saedi N, et al. Gut microbiota-derived tryptophan metabolites modulate inflammatory response in hepatocytes and macrophages. *Cell Rep*. 2018;23(4):1099-1111. https://doi.org/10.1016/j.celrep.2018.03.109.
58 Sugimoto Y, Kimura I, Yamada J, et al. The involvement of insulin in tryptamine-induced hypoglycemia in mice. *Life Sci*. 1991;48(17):1679-1683. https://doi.org/10.1016/0024-3205(91)90128-X.
59 Zhai L, Xiao H, Lin C, et al. Gut microbiota-derived tryptamine and phenethylamine impair insulin sensitivity in metabolic syndrome and irritable bowel syndrome. *Nat Commun*. 2023;14(1):4986. https://doi.org/10.1038/s41467-023-40552-y.
60 Kristensen SL, Rorth R, Jhund PS, et al. Cardiovascular, mortality, and kidney outcomes with GLP-1 receptor agonists in patients with type 2 diabetes: a systematic review and meta-analysis of cardiovascular outcome trials. *Lancet Diabetes Endocrinol*. 2019;7(10):776-785. https://doi.org/10.1016/S2213-8587(19)30249-9.
61 Tao X, Huang W, Pan L, et al. Optimizing *ex vivo* culture conditions to study human gut microbiome. *ISME Commun*. 2023;3(1):38. https://doi.org/10.1038/s43705-023-00245-5.

The cover presents diabetes as a systemic metabolic condition, represented by the silhouette of an obese body alongside a glucose meter that signals impaired glycemic control. The highlighted intestinal region reflects increasing recognition that gut microbial ecology and intestinal homeostasis are associated with metabolic balance. This framing emphasizes the gut as a place where microbial activity influences host physiology and contributes to metabolic regulation.

In the lower right, the illustration of *Magnolia officinalis* and its bark (Houpo) grounds the composition in the domain of natural product therapeutics. Honokiol, a major active constituent, is shown modulating *Akkermansia muciniphila* and enhancing its production of tryptamine metabolites that engage AHR signaling and stimulate GLP-1 secretion, ultimately supporting metabolic improvement in diabetes. Together, the imagery conveys an integrated concept: natural products can influence microbial activity and host metabolic signaling in ways that support metabolic health.